



1 **Role of nitrogen and iron biogeochemical cycles on the production and export**  
2 **of dissolved organic matter in agricultural headwater catchments**

3 Thibault Lambert<sup>1</sup>, Rémi Dupas<sup>1,\*</sup>, Patrick Durand<sup>1</sup>

4 <sup>1</sup> INRAE, UMR SAS 1069, L'Institut Agro, Rennes, France

5 \* Corresponding author

6 **Abstract**

7 To obtain better constraints on the control of the seasonal variations on dissolved organic  
8 carbon (DOC) export in lowland catchments, we combined monitoring of nitrates, iron,  
9 soluble phosphorus and dissolved organic matter concentration (as DOC) and composition  
10 (fluorescence) in soil and stream waters at a regular interval during one hydrological cycle.  
11 We installed 21 zero-tension lysimeters in in top soil organic-rich soil horizons (15 cm below  
12 the soil surface) in the riparian area of a well-monitored agricultural catchment in French  
13 Brittany and visited them with a weekly to biweekly frequency from October 2022 to June  
14 2023. We observed a large increase in DOC concentrations in riparian soils during the high  
15 flow period, notably due to the establishment of Fe-reducing conditions and the subsequent  
16 release of organic molecules in soil waters. We also noted that the timing and the spatial  
17 variability of Fe(II) biodissolution in soils was regulated by nitrates from agricultural origin and  
18 the heterogeneity of water flow paths at the catchment scale. Contrary to our current  
19 understanding of DOC export in headwater catchment, our results lead us to consider the  
20 winter high flow period as an active phase of both DOC production and export in headwater  
21 catchments.

22 **1. Introduction**

23 Dissolved organic matter (DOM) is a key component of the ecological and biogeochemical  
24 functioning of aquatic ecosystems (Hanson et al., 2015), affecting for instance light  
25 penetration (Kelly et al., 2001), pollutant transport (Aiken et al., 2011), aquatic microbial  
26 metabolism (Wetzel, 1992), and the treatment of drinking waters (Chow et al., 2005). Aquatic  
27 DOM, which is mainly of terrestrial origin, represents a fundamental link between the  
28 terrestrial, oceanic, and atmospheric compartments of the global carbon cycle (Dean et al.,  
29 2020; Battin et al., 2008). Unravelling the sources and drivers of DOM export has become an  
30 urgent environmental issue in a context of long-term increasing concentrations of dissolved  
31 organic carbon (DOC, a proxy for DOM content) reported in numerous streams in the  
32 northern hemisphere (Monteith et al., 2007; De Wit et al., 2021).



33 Headwater catchments are the main entry point of DOM into fluvial networks in temperate  
34 oceanic climate (Ågren et al., 2007) and riparian soils have been identified as the dominant  
35 sources of riverine DOM at the catchment scale owing to their location at the terrestrial-  
36 aquatic interface (Sanderman et al., 2009; Lambert et al., 2014). The flushing of shallow  
37 organic-rich soil layers during storm events represents the majority of annual DOC loads  
38 (Inamdar et al., 2006), and the DOC *versus* discharge relationships during storm events  
39 show that DOC export is transport-limited (Buffam et al., 2001; Zarnetske et al., 2018). At the  
40 annual scale, riparian soils act as a non-limited store (Hinton et al., 1998; Lambert et al.,  
41 2013), however the processes regulating the size of the pool of riparian DOM across  
42 seasons remain unclear.

43 DOC export at the annual scale is commonly conceptualized as a two-steps process in which  
44 DOM is produced and stored in the catchment during the hot and dry period, and then  
45 exported toward surface waters during the wet and cold period (Wen et al., 2020;  
46 Strohmenger et al., 2020; Tiwari et al., 2022; Ruckhaus et al., 2023; Deirmendjian et al.,  
47 2018). Antecedent soil conditions of wetness and temperature have been identified as a  
48 dominant control on stream DOC with concentrations typically increasing after dry events  
49 (Turgeon and Courchesne, 2008; Vázquez et al., 2007; Mehring et al., 2013). Periods of  
50 drought promote the production and accumulation of dissolved organic material in upper soil  
51 horizons through enhanced soil organic matter decomposition (Harrison et al., 2008; Fenner  
52 and Freeman, 2011; Xu and Saiers, 2010), resulting in high stream DOC concentrations  
53 during the subsequent rewetting phase of the catchment (Werner et al., 2019; Raymond and  
54 Saiers, 2010). In good agreement with this conceptual model is the observation based on  
55 long-term data that the mean annual DOC concentrations in streams can be related to the  
56 intensity and duration of preceding dry periods (Humbert et al., 2015; Tiwari et al., 2022).

57 However, the establishment of reducing conditions in riparian soils during the winter may  
58 have potential implications on our conceptualization of stream DOC export owing to the  
59 influence of redox conditions on the iron (Fe) cycle in soils. While particulate Fe-hydroxides  
60 absorb with a high affinity organic substances when oxidizing conditions prevail, the  
61 microbially-driven dissolution of Fe oxyhydroxides during reducing conditions led to the  
62 release of organic molecules previously bounded to surface minerals (Hagedorn et al., 2000;  
63 Blodau et al., 2008). The release of large amounts of DOM in riparian soils during the winter  
64 period – considered as passive (i.e., non-productive) in our current conceptualisation of  
65 stream DOC export – has been previously reported (Lambert et al., 2013; Lotfi-Kalahroodi et  
66 al., 2021), and several studies have suggested that iron redox cycles may play a major role  
67 on catchment DOM export (Knorr, 2013; Selle et al., 2019; Musolff et al., 2017). However,  
68 the impact of Fe reduction could be limited in terms of DOC export considering that reducing



69 conditions are favoured by the hydrological confinement of soil horizons involved and by their  
70 isolation from the inflow of oxidizing species such as oxygen and nitrates from upslope that  
71 may prevent the reductive dissolution of iron (McMahon and Chapelle, 2008; Christensen et  
72 al., 2000).

73 Because most of the studies investigating DOC export in headwater catchments rely on data  
74 collected in stream waters, the processes regulating the size of the mobile DOM pool in  
75 riparian soils and the interaction with other biogeochemical cycles remain largely unseen and  
76 we still lack studies investigating how processes occurring in soil waters reflect our  
77 conceptualization of solutes dynamics based on observations made in surface waters. In this  
78 study, we investigated the potential influence of Fe redox cycles on stream DOC dynamics in  
79 an agricultural headwater catchment. More specifically, we tested the hypothesis that the  
80 controls of Fe reduction in riparian soils could affect significantly the export of DOC at the  
81 annual scale. Among these controls, we intended to pay particular attention to the dynamics  
82 of  $\text{NO}_3^-$  inflow from upslope. To this end, zero-tension lysimeters were installed in the riparian  
83 area of a well-instrumented agricultural catchment located in Brittany (France) that shows a  
84 low but significant increase in stream DOC concentrations over the last decades  
85 (Strohenger et al., 2020). The variations of soil solution chemistry during the 2022-2023  
86 hydrological cycle was tracked. We measured DOC, Fe(II) and  $\text{NO}_3^-$  concentrations but also  
87 DOM composition (absorbance and fluorescence properties coupled with parallel factor  
88 analysis) and soluble reactive phosphorus (SRP) as an additional tracer of Fe reductive  
89 dissolution (Gu et al., 2017; Smith et al., 2021). The results allowed us to decipher complex  
90 interactions across C, N, and Fe cycles in agricultural catchments and to highlight the  
91 occurrence of several processes sustaining DOM export during the winter period.

## 92 **2. Material and method**

### 93 **2.1. Study site**

94 The Kervidy-Naizin research observatory is a 4.9-km<sup>2</sup> agricultural headwater catchment  
95 located in Brittany (western France, Fig. 1). It belongs to the French Critical Zone  
96 Observatories (OZCAR) network and is instrumented since the 1970s for the long-term  
97 monitoring of the soil-atmosphere-hydrosphere continuum in a context of intensive  
98 agriculture (see Fovet et al., 2018 for a complete presentation of the study site).

99 The site is characterized by gentle slopes (<5%) and low elevation that ranges from 98–140  
100 m above sea level. The bedrock is composed of impermeable Brioverian schists above which  
101 a locally fractured layer of schists is overlaid by 1 – 30 m of weathered material and silty  
102 loam soils. Soils are well drained except in riparian zones, where water excess leads to  
103 hydromorphic, poorly drained soil. The land use is intensive mixed farming, with 91% of the



104 watershed area under agriculture that grows crops to feed a high density of dairy cattle, pigs  
105 and poultry.. The watershed area is dominated by maize (38%), straw cereals (30%), and  
106 grasslands (15%), and wooded areas are mainly confined to valley bottoms along the stream  
107 channel or to some hedgerows along fields (Fig. 1).

108 The climate is temperate oceanic, with mean annual temperature of  $11.2 \pm 0.6^\circ\text{C}$  and mean  
109 annual precipitation of  $810 \pm 180$  mm. Precipitation varies seasonally throughout the year,  
110 with higher precipitation from October to February (mean monthly precipitation of  $92 \pm 31$   
111 mm) and lower precipitation from March to July (mean monthly precipitation of  $50 \pm 14$  mm).  
112 The dynamics of the draining stream, called the Coët Dan, reflects the seasonal pattern of  
113 rainfall and evapotranspiration with high discharge periods from November to April and  
114 completely dry periods from July to October depending on hydrological years.

115 Groundwater level fluctuations are recorded every 15 min along the Kerolland (K) transect,  
116 rainfall is monitored at hourly intervals using a weather station located ~ 1400 m from the  
117 catchment outlet, and stream discharge is recorded every minute with an automatic gauge  
118 station at the outlet of the catchment. A S::SCAN probe is installed at the outlet of the  
119 catchment for the measurement of DOC and other variables at high-frequency (Fovet et al.,  
120 2018).

## 121 **2.2. Monitoring and manual sampling**

122 We investigated the seasonal variability of the riparian DOM pool using zero-tension  
123 lysimeters installed in September 2022 in topsoil organic horizons (15 cm depth) in the  
124 Kerrolland riparian zone, an area known to be a major contributor of stream DOC export in  
125 this catchment (Lambert et al., 2014). Lysimeters were randomly installed at different  
126 distances from the stream channel with the aim to capture different water flowpaths with  
127 different degrees of nitrate concentrations. In total, 29 zero-tension lysimeters were installed,  
128 but some were lost during the study period because of degradation by rodents. We retained  
129 lysimeters for which at least seven consecutive dates of data were available, resulting in 17  
130 lysimeters used for the study. We collected soil waters from November 2022 to June 2023 at  
131 a frequency ranging from 2 to 4 visits per month depending on the hydro-climatic conditions  
132 (Fig. 1). The end of sampling was imposed by the lack of water in lysimeters owing to the  
133 gradual drawdown of the water table in the riparian zone during the spring. Soil waters were  
134 collected with a vacuum pump and filtered at  $0.2 \mu\text{m}$  with acetate cellulose syringe  
135 encapsulated filters directly on site for all analyses including DOC,  $\text{NO}_3^-$ , SRP, Fe(II), and  
136 DOM composition. Unfiltered water was used to measure basic physico-chemistry variables  
137 including temperature and pH with an ODEON probe (XXX). In addition, surface waters were



138 collected right next to the riparian area where lysimeters were installed and at the outlet of  
139 the catchment. The laboratory analyses were identical for soil and surface waters.

### 140 **2.3. Analytical procedures**

141 With the exception of Fe(II) measurements that were performed the same day as sampling,  
142 all analyses were done within two weeks after sampling. Samples were stored in a 4°C cold  
143 room in the dark. Fe(II) analyses were determined using the 1,10-phenanthroline colorimetric  
144 method (Lambert et al., 2013): dissolved iron was trapped on site and the optical density of  
145 the complex formed with phenanthroline was measured the same day once back to the  
146 laboratory at 510 nm with an UV-vis spectrophotometer (XXX). DOC concentrations were  
147 measured using a total carbon analyzer (SHIMADZU TOC-V) with a precision estimated at ±  
148 5% using a standard potassium hydrogen phthalate solution (SIGMA ALDRICH). NO<sub>3</sub><sup>-</sup> and  
149 SRP were determined by spectrometry with an automatic sequential analyzer (SmartChem  
150 200, AMS Alliance, France).

151 Absorbance for colored DOM (CDOM) was measured with a Lambda 365 UV/vis  
152 spectrophotometer (Perkin Elmer) from 200 to 700 nm (1 nm increment) using a 1 cm quartz  
153 cuvette. CDOM spectra were used to correct excitation-emission matrices (EEMs) for inner  
154 filter effects (Ohno, 2002). Fluorescence DOM (FDOM) was collected as EEMs with a  
155 Lambda LS45 (Perkin Elmer) using a 1 cm quartz cuvette across excitation wavelengths of  
156 270 – 450 nm (5 nm increment) and emission wavelengths of 290 – 600 nm (0.5 nm  
157 increment). Samples were diluted in most case to reduce inner filter effects and iron  
158 quenching. Usual DOM absorbance and fluorescence indices such as specific UV  
159 absorbance or slope ratio were not calculated because of they are sensitive to the presence  
160 of iron (Logozzo et al., 2022) while the deconvolution of EEMs through parallel factor  
161 analysis (PARAFAC) is not (Poulin et al., 2014).

### 162 **2.4. PARAFAC modelling**

163 EEMs preprocessing (Raman scattering removal and standardization to Raman units) was  
164 performed prior to the PARAFAC modeling. Normalization was done using a Milli-Q water  
165 sample run the same day as the sample. A five-component PARAFAC model was obtained  
166 using the drEEM 0.3.0 Toolbox (Murphy et al., 2013) for MATLAB (MathWorks, Natick, MA,  
167 USA). Split-half analysis, random initialization, and visualization of residuals EEMs were  
168 used to test and validate the model. The positions of maximum peaks of the PARAFAC  
169 components were compared to previous studies carried out in similar context of human-  
170 impacted catchments with the open fluorescence database OpenFluor using the OpenFluor  
171 add-on for the open-source chromatography software OpenChrom (Murphy et al., 2014). The  
172 maximum fluorescence  $F_{\text{Max}}$  values of each component for a particular sample provided by



173 the model were summed to calculate the total fluorescence signal  $F_{Tot}$  of the sample in  
174 Raman units. The relative abundance of any particular PARAFAC component  $X$  was then  
175 calculated as  $\%C_X = F_{Max}(X)/F_{Tot}$ .

## 176 **2.5. Statistical analyses**

177 A principal component analysis (PCA) coupled with a cluster analysis was performed to  
178 identify and group lysimeters having similar patterns. Data used included the mineral  
179 composition of soil waters (i.e. DOC,  $NO_3^-$ , SRP and Fe(II) concentrations) as well as the  
180 composition of DOM based on PARAFAC results (i.e. PARAFAC components). Data for  
181 each lysimeters were first averaged and then normalized. The PCA was performed using the  
182 *prcomp* function in the R software, and the *factoextra* package was used to identify the  
183 variables that contribute the most to the first two dimensions of the PCA. The cluster  
184 analysis, based on the results from the PCA and called Hierarchical Clustering on Principal  
185 Components (Josse, 2010), was performed with the *FactoMineR* package for R (Lê et al.,  
186 2008).

## 187 **3. Results**

### 188 **3.1. Hydro-climatic context**

189 The hydrological regime of small temperate catchments developed above fractured substrate  
190 such as Kervidy-Naizin is characterized by several three distinct successive periods  
191 determined by groundwater fluctuations (Fig. 2A-B). The first period (01/09/2022 –  
192 17/12/2022) corresponds to the rewetting phase of the catchment after the dry summer  
193 season: moderate precipitations ( $5.1 \pm 5.3$  mm  $d^{-1}$ , cumulated precipitation = 338.5 mm)  
194 progressively lead to the rise of groundwater first in the riparian zone and then in upland  
195 domain but stream discharge remains low owing to a low groundwater table. The second  
196 period (18/12/2022 – 15/05/2023) corresponds to the high flow period initialized by the rise of  
197 the water table in upland soils. Frequent and intense rainfall events maintained a high stream  
198 flow, except during several weeks without significant precipitations (17/01/2023 –  
199 06/03/2023,  $2.1 \pm 4.5$  mm  $d^{-1}$ , cumulated precipitation = 23 mm). Although stream flow  
200 declined significantly, the water table remained close to the surface and riparian soils  
201 remained waterlogged. Finally, the third period (16/05/2023 – 01/07/2023) corresponds to the  
202 gradual drawdown of the water table in the catchment owing to rarer and scattered  
203 precipitations associated with higher temperature and evapotranspiration rates. Air  
204 temperature (Fig. 2C) showed a smoothed seasonal variability with decreasing values from  
205 September to December (from  $\sim 20^\circ C$  to  $-2^\circ C$ ) followed by a rise in temperature from  $0^\circ C$  to  
206  $20^\circ C$  from February to July. This pattern was only interrupted by a relatively short episode of



207 temperature close to 10°C during the winter, higher than usual temperature at this period,  
208 coinciding with the first intense rainfall period of the year.

### 209 **3.2. Fluorescence properties of DOM**

210 Five PARAFAC components were identified in soil solutions (Supplementary Fig. S1), all of  
211 which already described in previous studies. All five components had humic-like fluorescence  
212 properties (Fellman et al., 2010). Components C1 (excitation/emission peaks = 350 nm /444  
213 nm), C2 (<270/450), and C5 (410/488) predominantly cover the regions of EEMs associated  
214 with peaks A and C and are common tracers of terrestrially-derived DOM in surface waters  
215 (Kothawala et al., 2015; Stedmon and Markager, 2005; Logozzo et al., 2023; Lambert et al.,  
216 2017) while C3 (330/406) and C4 (295/410) are both located near the classical peak M,  
217 indicating a microbial transformation of terrestrial DOM (Williams et al., 2010; Lambert et al.,  
218 2022; Yamashita et al., 2010). The maximum fluorescence intensity of all components were  
219 strongly related to DOC concentrations (not shown) and the relative contribution of each  
220 component decreased from as C1 (29.7±3.1%) > C2 (28.3±3.6%) > C3 (19.5±2.5%) > C4  
221 (12.9±6.6%) > C5 (9.7±2.1%).

### 222 **3.3. Overview of the seasonal variations in soil and stream waters**

223 Temperature in soil waters (Fig. 3A) followed the same pattern as air temperature: values  
224 oscillated from 5°C to 15°C during November – January, reached minimums between 4 and  
225 7 °C in January – March and then increased gradually during the rest of the study period up  
226 to 18 – 20 °C in June. pH varied from 6.2 to 7.4 (mean 6.9 ± 0.3) across lysimeters and didn't  
227 exhibit significant trends over the study period (Fig. 3B). Solutes, however, exhibited complex  
228 patterns with a high variability across lysimeters and time, especially during the high flow  
229 period (Fig. 3C-F). Overall, these elements were strongly linked to each other (Fig. 4). DOC  
230 concentrations ranged from 2.3 to 87.4 mg L<sup>-1</sup> (mean = 30.2±12.8 mg L<sup>-1</sup>) over the study  
231 period and were linearly and positively associated with Fe(II) that ranged from 0 to 45.8 mg L<sup>-1</sup>  
232 <sup>1</sup> (mean = 9.8±7.6 mg L<sup>-1</sup>). Fe(II) was negatively correlated with NO<sub>3</sub> (from 0 to 16.4 mg L<sup>-1</sup>,  
233 mean = 0.9±1.1 mg L<sup>-1</sup>), and SRP (from 0 to 0.5 mg L<sup>-1</sup>, mean = 0.1±0.1 mg L<sup>-1</sup>) was also  
234 positively related to Fe(II), but not as strongly as for DOC. Some lysimeters, however, did not  
235 followed these relationships and showed some variations in DOC and SRP concentrations  
236 but no significant Fe(II) concentrations.

237 Stream DOC was highly variable, ranging from 2.9 to 36.8 mg L<sup>-1</sup> (Fig. 7), and reached its  
238 maximum concentrations during rainfall events as subsurface flows flush DOM-rich waters  
239 from the riparian area (Lambert et al., 2011). Maximum and minimum concentrations trended  
240 downwards from December to March but concentrations at peak discharge showed an



241 increasing pattern from March to May, a feature resembling that displayed by soil waters  
242 from the riparian area.

### 243 **3.4. PCA and cluster analysis**

244 Overall, the two first components of the PCA explained 69.4 % of the variance and  
245 discriminated lysimeters depending on the degree of Fe(II) biodissolution in soil waters  
246 occurring in the riparian zone of the Kervidy-Naizin catchment (Fig. 5). The first principal  
247 component (PC1, 54% of the total variance) mainly related to NO<sub>3</sub> concentrations and  
248 terrestrial humic-like components (C1, C2, and C5) on positive scores, and to DOC and  
249 Fe(II) concentrations and the microbial humic-like component C4 on negative scores. The  
250 second component (PC2, 15.4% of the total variance) was related to SRP (positive score)  
251 and the component C3 (negative score). In other words, lysimeters capturing Fe(II)  
252 biodissolution in the riparian area were associated with high DOC and a greater proportion of  
253 C4 component compared to lysimeters enriched in nitrates where no Fe(II) was measured.

254 The hierarchical clustering based on the PCA results grouped the lysimeters in two distinct  
255 clusters based on the presence (cluster 1) or absence (cluster 2) of Fe(II) (Fig. 5). This  
256 approach allowed us to gain more precise insights into the temporal evolution of solutes in  
257 soil solutions since clear patterns appeared once the data were grouped by cluster (Fig. 6).  
258 Hence, soil solutions grouped in cluster 1 showed an initial flushing dynamic for all elements  
259 except Fe(II) that was almost absent from soil solutions during the rewetting phase of the  
260 catchment. Iron reductive biodissolution was triggered during the high flow period in January,  
261 at a moment when soil solutions were depleted in nitrate. Then, Fe(II) concentrations showed  
262 a gradual increase up to  $26.3 \pm 10.3 \text{ mg L}^{-1}$  until the drawdown of the water table and the  
263 consecutive aeration of riparian soils in June led Fe(II) to quickly decrease below  $10 \text{ mg L}^{-1}$ .  
264 This increasing pattern was interrupted during a short period in February – March, *i.e.* during  
265 the ‘dry’ period of the winter, during which Fe(II) dropped from  $16.6 \pm 9.6 \text{ mg L}^{-1}$  to  $9.1 \pm 4.5 \text{ mg}$   
266  $\text{L}^{-1}$  before starting again to rise. DOC and SRP both followed a similar trend as Fe(II):  
267 concentrations gradually raised from January to the end of March up to  $54.9 \pm 25.0 \text{ mg L}^{-1}$  and  
268  $0.18 \pm 0.11 \text{ mg L}^{-1}$ , respectively, and then dropped to  $17.5 \pm 10.9 \text{ mg L}^{-1}$  and  $0.02 \pm 0.02 \text{ mg L}^{-1}$   
269 in June, respectively.

270 Soil solutions from the second cluster also showed a flushing pattern, however it lasted  
271 longer than soil solutions from the first cluster and concerned only DOC and SRP. Indeed,  
272 while NO<sub>3</sub> concentrations decreased in lysimeters from cluster 1, it increased in lysimeters  
273 from cluster 2. These patterns of decreasing DOC (from  $34.5 \pm 7.1 \text{ mg L}^{-1}$  to  $< 10 \text{ mg L}^{-1}$ ) and  
274 SRP (from  $0.19 \pm 0.08 \text{ mg L}^{-1}$  to  $< 0.02 \text{ mg L}^{-1}$ ) but increasing NO<sub>3</sub> (from  $0.57 \pm 0.81 \text{ mg L}^{-1}$  to ~  
275  $8 \text{ mg L}^{-1}$ ) lasted until the middle of February/beginning of March. After that, DOC and SRP





276 increased up to  $> 20 \text{ mg L}^{-1}$  and  $0.16 \text{ mg L}^{-1}$  (but note that SRP dropped close to depletion at  
277 the end of the monitoring), respectively, while  $\text{NO}_3$  decreased until a complete depletion at  
278 the beginning of the recession period of the water table. In these lysimeters, Fe(II) was not  
279 measured at significant concentrations (*i.e.* remained below  $0.5 \text{ mg L}^{-1}$ ) except in March,  
280 during which Fe(II) increased from  $1.2 \pm 1.9$  to  $4.1 \pm 0.2 \text{ mg L}^{-1}$ .

## 281 4. Discussion

### 282 4.1. The buffering effect of nitrates on iron reductive dissolution

283 The reductive biodissolution of iron during the high-water winter period is a recurrent process  
284 in riparian soils of headwater catchments (Škerlep et al., 2023; Smolders et al., 2017) and  
285 the amplitudes of variations in Fe(II) and associated DOC and SRP dynamics reported in this  
286 study are in line with previous works conducted in the same research catchment (Lambert et  
287 al., 2013; Lotfi-Kalahroodi et al., 2021; Gu et al., 2017). Our results, however, clearly  
288 evidenced a marked variability in the intensity of iron dissolution across lysimeters that we  
289 attributed to the spatial distribution of  $\text{NO}_3$ -rich water flow paths that can inhibit and delay the  
290 apparition of Fe(II) (and DOC) in soil solutions.

291 A fundamental condition for the establishment of reductive conditions is the prolonged  
292 waterlogging of riparian soils. As shown earlier for this and other lowland catchments on  
293 impervious bedrock, the higher hydraulic gradient induced by the rise of the upland  
294 groundwater level during winter maintains a strong hydrologic connection between upland  
295 and riparian domains (Pacific et al., 2010; Molenat et al., 2008). Under these conditions,  
296 riparian soils remained waterlogged even during low-precipitation moments as long as the  
297 water table level remained elevated in upland areas (Fig. 2). Soil horizons may therefore  
298 remain waterlogged, leading to the establishment of reductive conditions as long as inputs of  
299 oxidizing species remained limited and/or counterbalanced by higher rate of consumption  
300 through microbial activity. This pattern was well illustrated by records from lysimeters  
301 grouped in the first cluster (Fig. 6). After a quick depletion of an initial stock of nitrate  
302 accumulated during the previous summer, reductive conditions were rapidly established  
303 during the winter period and Fe-biodissolution was triggered. The increase in Fe(II)  
304 concentrations during January implies that precipitation events were not intense enough to  
305 provide oxygen to soil waters while the slight decrease observed during the February/March  
306 period illustrates the influence of the hydraulic gradient in regulating reductive conditions in  
307 riparian soils. As a direct consequence, DOC and SRP showed an increasing pattern in soil  
308 waters from December to May but abruptly decreased in June as riparian soils became  
309 aerated. The restoration of aerobic conditions owing to the drawdown of the water table in



310 the bottomland domain led to the formation of Fe-minerals and the subsequent retention of  
311 DOC and SRP (Gu et al., 2017).

312 Lysimeters included in the second cluster showed a very different pattern. Although some of  
313 them were located close (< 1m) to lysimeters in which reducing conditions prevailed, there  
314 was no evidence of Fe(II) release owing to the presence of nitrate in soil waters. Indeed, and  
315 in agreement with studies carried out in wetland (Lucassen et al., 2004) and lacustrine  
316 (Andersen, 1982) sediments, we argued that the Fe-biodissolution was  
317 inhibited as long as long as NO<sub>3</sub> remained in sufficient quantity in soil waters. In the absence  
318 of such mobilization or regeneration process, both DOC and SRP showed a net depletion  
319 pattern from November to March. The influence of nitrate as a buffer of Fe-biodissolution was  
320 furthermore supported by the observation of a slight release of Fe(II) in May, at a moment  
321 when nitrate became depleted from soil waters, probably because of plant uptake.  
322 Interestingly, we found that the threshold value of nitrates above which the process is  
323 activated (based on the nitrates *versus* Fe(II) relationship (Fig. 4) as well as timing of Fe-  
324 biodissolution identified in cluster 1 and cluster 2) ranged between 1.2 and 1.8 N-NO<sub>3</sub> (4.1 –  
325 6.2 mg L<sup>-1</sup>), which is close to the threshold value of 6 mg L<sup>-1</sup> reported by Musolff et al., 2017  
326 in German streams.

327 Our study evidences a strong spatial heterogeneity of the establishment of reducing  
328 conditions in the riparian area of the Kervidy-Naizin catchment, associated with differences in  
329 the composition of DOM released in soil solutions. The PARAFAC components identified in  
330 the model pointed to a dominance of highly aromatic and conjugated molecules, typical of  
331 DOM derived from soil organic matter and found in poorly drained soils in riparian or wetland  
332 areas (Sanderman et al., 2009; Lambert et al., 2013; Yamashita et al., 2010). A greater  
333 proportion of the C4 component within the DOM pool was found in soil waters under reducing  
334 conditions, indicating a greater proportion of microbially-derived DOM that we associated  
335 with the microbial reduction of Fe oxyhydroxides. It remain to be determined, however, the  
336 reason for such variability in biogeochemical processes occurring in riparian soils. A first  
337 explanation can be related to the water circulation in soils. In intensive agricultural  
338 catchments such as our study site, inflow of NO<sub>3</sub>-rich water may arise from the rise of  
339 contaminated groundwater in valley bottom s and/or from subsurface flow paths that connect  
340 upland soils to riparian soils (Molenat et al., 2008). It is likely that lysimeters from the second  
341 cluster captured preferential flow paths of NO<sub>3</sub>-rich waters while lysimeters from the first  
342 cluster were disconnected from those preferential water circulations. Alternatively, the  
343 absence of nitrates in soil waters may arise from a higher rate of denitrification that  
344 counterbalanced NO<sub>3</sub> inputs. Research based on field observation remained limited to  
345 decipher the respective role of hydrology *versus* biogeochemistry in controlling Fe(II)



346 biodissolution in riparian soils, and experimental studies would be required to provide more  
347 quantitative values on these potential drivers and their interactions.

#### 348 **4.2. Implication on stream DOM export at the catchment scale**

349 The current understanding of DOM export in lowland headwater catchments is based on a  
350 two-steps conceptual model according to which the pool of DOM is built in soils during a low  
351 hydrological connectivity period and then flushed toward surface waters during the following  
352 high flow period (e.g. Tiwari et al., 2022; Ruckhaus et al., 2023; Strohmenger et al., 2020;  
353 Raymond and Saiers, 2010). Although the decline in DOC concentrations in soil waters from  
354 cluster 2 between November and mid-February and to a lesser extent in soil waters in cluster  
355 1 from November to mid-December are in good agreement with this view, the general  
356 increase in DOC in all lysimeters between March and May now leads us to consider the high  
357 flow period as an active phase of both production and export.

358 We know from isotopic studies that riparian soils where we installed our lysimeters are the  
359 dominant source of DOM at the catchment scale (Lambert et al., 2014). The contribution of  
360 uppermost soil horizons of riparian areas has been estimated between 80-90% of stream  
361 DOC fluxes due to the formation of shallow flow paths that connect soil and stream waters  
362 during storm events (Lambert et al., 2014). This previous knowledge is consistent with the  
363 observation that stream DOC variability closely reflected the temporal dynamics of DOC  
364 measured in soil waters (Fig.s 6 and 7). The general decrease of stream DOC during base  
365 flow and at peak discharge from November to February illustrated well the mobilisation and  
366 exhaustion of an initial supply-limited pool of DOM built during the summer period (Humbert  
367 et al., 2015). The general flushing behaviour of the catchment at this moment was illustrated  
368 by the strong decrease of DOC and SRP observed in soils from cluster 2 that became almost  
369 depleted in February-March (Fig. 6). On the other hand, the rapid onset of Fe biodissolution  
370 in some areas of the riparian domain (cluster 1) sustained DOM export and likely explained  
371 why stream DOC concentrations at peak discharge remained stable across successive  
372 storms in January (Fig. 7).

373 Conversely, the increase in DOC in soil solutions in the valley bottoms during the second  
374 high flow period have two important implications regarding our conceptualisation of DOM  
375 export in headwater catchments. First, it challenges the idea that the wet period acts mainly  
376 as a passive exportation period for DOC, with no or little DOC production (Strohmenger et  
377 al., 2020; Ruckhaus et al., 2023; Wen et al., 2020). The large two to three fold increase in  
378 DOC concentrations in riparian soils (in cluster 1 and 2, respectively) denotes a large  
379 mobilisation of DOM despite wet and low temperature conditions with significant  
380 consequences on stream DOC fluxes. Indeed, the gradual regeneration of the riparian DOM



381 pool was well reflected in stream DOC, whose concentrations at peak discharge showed an  
382 increasing trend across successive storm events from March to May (Fig. 7). Secondly, the  
383 release of large amount of DOM in lysimeters of cluster 2 where Fe(II) did not increase  
384 implies that several production mechanisms other than iron biodissolution can produce or  
385 regenerate the pool of riparian DOM. It is unlikely that agricultural inputs (crop residues,  
386 manure application, etc) main may explain the increases in the riparian area, as these  
387 sources are episodic and/or size-limited (Lambert et al., 2014; Humbert et al., 2015; Pacific  
388 et al., 2010). The highly aromatic nature of DOM strongly supports our assessment that the  
389 rise of DOM is due to a “local” production rather than external inputs. This observation echoes  
390 previous works on the Kervidy-Naizin catchment showing effective interannual regeneration  
391 mechanisms of the pool of soluble phosphorus in soils unrelated to iron dynamics (Gu et al.,  
392 2017), a statement supported here by the fact that SRP concentrations followed a similar  
393 pattern as DOC in soils grouped in the second cluster (Fig. 6). Unfortunately, we do not have  
394 the necessary data such as isotopes or molecular markers to elucidate the precise origin and  
395 DOM (and SRP) release in soils unrelated to iron biodissolution, and this should be the focus  
396 of future work combining experimental and field studies.

### 397 **Conclusion**

398 The combined monitoring of soil and stream waters in a lowland headwater catchment  
399 allowed us to evidence the dual role of high flow period as both an active phase of DOC  
400 production and export. The establishment of Fe-reducing conditions in riparian areas was  
401 identified as a major mechanism for stream DOC export, but our study also highlighted the  
402 buffering role of nitrates that could delay the release of large amount of DOM in soils,  
403 spatially and temporally.

404 The interactions between N and Fe biogeochemical cycles may have potential implications  
405 regarding the reasons for long-term increases in DOC in streams of Brittany. Indeed, stream  
406 DOC in the Kervidy-Naizin catchment has been slowly but significantly increasing in the last  
407 two decades, and this trend is mirrored by a decline in NO<sub>3</sub> concentrations (Strohmenger et  
408 al., 2020). While part of the DOC trend can be related to changes in climatic conditions as  
409 winters tend to wetter over the years, the long-term decline in N inputs from agriculture may  
410 have favoured the increase in stream DOC by enhancing Fe(II) biodissolution in riparian  
411 soils. If this was verified, it could partly explain why catchments having similar  
412 geomorphological and climatic properties present contrasting long-term trends at the scale of  
413 the Brittany region (Supplementary Fig. S2). Indeed, nitrate concentrations have largely  
414 decreased during the last decades, but the rate of recovery is not uniform across the region  
415 (Abbott et al., 2018). Studies carried out at the regional scale aiming to decipher the



416 interactions between local (agricultural practices) and global (climatic conditions) and the  
417 consequences on stream DOC export would be critical considering the influence of DOM on  
418 water quality and on the ecological and biogeochemical functioning of surface waters.

#### 419 **Data availability**

420 Data on soil solutions will be published on Zenodo.org upon the reservation that the paper  
421 will be accepted for publication. Hydrological and climatic data from the Kervidy-Naizin site  
422 are available here: [https://geosas.fr/web/?page\\_id=103](https://geosas.fr/web/?page_id=103).

#### 423 **Acknowledgements**

424 We thank Militza G., Harald F., P. Petitjean and Celine B. for their assistance in field and lab  
425 work.

#### 426 **Financial support**

427 This project has received funding from the H2020 European Research Council under the Marie  
428 Skłodowska-Curie grant agreement COSTREAM No 101064945.

#### 429 **Author contribution**

430 TL conceived the study, collected field samples and made laboratory analysis. TL drafted the  
431 manuscript with inputs from RD. All authors contributed to the manuscript.

#### 432 **Competing interests**

433 The authors declare that they have no conflict of interest.

#### 434 **References**

- 435 Abbott, B. W., Moatar, F., Gauthier, O., Fovet, O., Antoine, V., and Ragueneau, O.: Trends and seasonality of river nutrients in  
436 agricultural catchments: 18years of weekly citizen science in France, *Science of The Total Environment*, 624, 845-858,  
437 <https://doi.org/10.1016/j.scitotenv.2017.12.176>, 2018.
- 438 Ågren, A., Buffam, I., Jansson, M., and Laudon, H.: Importance of seasonality and small streams for the landscape regulation of  
439 dissolved organic carbon export, *Journal of Geophysical Research: Biogeosciences*, 112,  
440 <https://doi.org/10.1029/2006JG000381>, 2007.
- 441 Aiken, G. R., Hsu-Kim, H., and Ryan, J. N.: Influence of Dissolved Organic Matter on the Environmental Fate of Metals,  
442 Nanoparticles, and Colloids, *Environmental Science & Technology*, 45, 3196-3201, 10.1021/es103992s, 2011.
- 443 Andersen, J. M.: Effect of nitrate concentration in lake water on phosphate release from the sediment, *Water Research*, 16, 1119-  
444 1126, [https://doi.org/10.1016/0043-1354\(82\)90128-2](https://doi.org/10.1016/0043-1354(82)90128-2), 1982.
- 445 Battin, T. J., Kaplan, L. A., Findlay, S., Hopkinson, C. S., Marti, E., Packman, A. I., Newbold, J. D., and Sabater, F.: Biophysical  
446 controls on organic carbon fluxes in fluvial networks, *Nature Geoscience*, 1, 95-100, 10.1038/ngeo101, 2008.
- 447 Blodau, C., Fulda, B., Bauer, M., and Knorr, K.-H.: Arsenic speciation and turnover in intact organic soil mesocosms during  
448 experimental drought and rewetting, *Geochimica et Cosmochimica Acta*, 72, 3991-4007,  
449 <https://doi.org/10.1016/j.gca.2008.04.040>, 2008.
- 450 Buffam, I., Galloway, J. N., Blum, L. K., and McGlathery, K. J.: A stormflow/baseflow comparison of dissolved organic matter  
451 concentrations and bioavailability in an Appalachian stream, *Biogeochemistry*, 53, 269-306, 10.1023/A:1010643432253,  
452 2001.
- 453 Chow, A. T., Gao, S., and Dahlgren, R. A.: Physical and chemical fractionation of dissolved organic matter and trihalomethane  
454 precursors: A review, *Journal of Water Supply: Research and Technology-Aqua*, 54, 475-507, 10.2166/aqua.2005.0044,  
455 2005.
- 456 Christensen, T. H., Bjerg, P. L., Banwart, S. A., Jakobsen, R., Heron, G., and Albrechtsen, H.-J.: Characterization of redox  
457 conditions in groundwater contaminant plumes, *Journal of Contaminant Hydrology*, 45, 165-241,  
458 [https://doi.org/10.1016/S0169-7722\(00\)00109-1](https://doi.org/10.1016/S0169-7722(00)00109-1), 2000.
- 459 de Wit, H. A., Stoddard, J. L., Monteith, D. T., Sample, J. E., Austnes, K., Couture, S., Fölster, J., Higgins, S. N., Houle, D., Hruška,  
460 J., Krám, P., Kopáček, J., Paterson, A. M., Valinia, S., Van Dam, H., Vuorenmaa, J., and Evans, C. D.: Cleaner air reveals



- 461 growing influence of climate on dissolved organic carbon trends in northern headwaters, *Environmental Research Letters*, 16,  
462 104009, 10.1088/1748-9326/ac2526, 2021.
- 463 Dean, J. F., Meisel, O. H., Martyn Rosco, M., Marchesini, L. B., Garnett, M. H., Lenderink, H., van Logtestijn, R., Borges, A. V.,  
464 Bouillon, S., Lambert, T., Röckmann, T., Maximov, T., Petrov, R., Karsanaev, S., Aerts, R., van Huissteden, J., Vonk, J. E.,  
465 and Dolman, A. J.: East Siberian Arctic inland waters emit mostly contemporary carbon, *Nature Communications*, 11, 1627,  
466 10.1038/s41467-020-15511-6, 2020.
- 467 Deirmendjian, L., Loustau, D., Augusto, L., Lafont, S., Chipeaux, C., Poirier, D., and Abril, G.: Hydro-ecological controls on  
468 dissolved carbon dynamics in groundwater and export to streams in a temperate pine forest, *Biogeosciences*, 15, 669-691,  
469 10.5194/bg-15-669-2018, 2018.
- 470 Fellman, J. B., Hood, E., and Spencer, R. G. M.: Fluorescence spectroscopy opens new windows into dissolved organic matter  
471 dynamics in freshwater ecosystems: A review, *Limnology and Oceanography*, 55, 2452-2462,  
472 <https://doi.org/10.4319/lo.2010.55.6.2452>, 2010.
- 473 Fenner, N. and Freeman, C.: Drought-induced carbon loss in peatlands, *Nature Geoscience*, 4, 895-900, 10.1038/ngeo1323,  
474 2011.
- 475 Fovet, O., Ruiz, L., Gruau, G., Akkal, N., Aquilina, L., Busnot, S., Dupas, R., Durand, P., Faucheux, M., Fauvel, Y., Fléchar, C.,  
476 Gilliet, N., Grimaldi, C., Hamon, Y., Jaffrezic, A., Jeanneau, L., Labasque, T., Le Henaff, G., Mérot, P., Molénat, J., Petitjean,  
477 P., Pierson-Wickmann, A.-C., Squidvidant, H., Viaud, V., Walter, C., and Gascuel-Odoux, C.: AgrHyS: An Observatory of  
478 Response Times in Agro-Hydro Systems, *Vadose Zone Journal*, 17, 180066, <https://doi.org/10.2136/vzj2018.04.0066>, 2018.
- 479 Gu, S., Gruau, G., Dupas, R., Rumpel, C., Crème, A., Fovet, O., Gascuel-Odoux, C., Jeanneau, L., Humbert, G., and Petitjean,  
480 P.: Release of dissolved phosphorus from riparian wetlands: Evidence for complex interactions among hydroclimate variability,  
481 topography and soil properties, *Science of The Total Environment*, 598, 421-431,  
482 <https://doi.org/10.1016/j.scitotenv.2017.04.028>, 2017.
- 483 Hagedorn, F., Kaiser, K., Feyen, H., and Schleppe, P.: Effects of Redox Conditions and Flow Processes on the Mobility of Dissolved  
484 Organic Carbon and Nitrogen in a Forest Soil, *Journal of Environmental Quality*, 29, 288-297,  
485 <https://doi.org/10.2134/jeq2000.00472425002900010036x>, 2000.
- 486 Hanson, P. C., Pace, M. L., Carpenter, S. R., Cole, J. J., and Stanley, E. H.: Integrating Landscape Carbon Cycling: Research  
487 Needs for Resolving Organic Carbon Budgets of Lakes, *Ecosystems*, 18, 363-375, 10.1007/s10021-014-9826-9, 2015.
- 488 Harrison, A. F., Taylor, K., Scott, A., Poskitt, J., Benham, D., Grace, J., Chaplow, J., and Rowland, P.: Potential effects of climate  
489 change on DOC release from three different soil types on the Northern Pennines UK: examination using field manipulation  
490 experiments, *Global Change Biology*, 14, 687-702, <https://doi.org/10.1111/j.1365-2486.2007.01504.x>, 2008.
- 491 Hinton, M. J., Schiff, S. L., and English, M. C.: Sources and flowpaths of dissolved organic carbon during storms in two forested  
492 watersheds of the Precambrian Shield, *Biogeochemistry*, 41, 175-197, 10.1023/A:1005903428956, 1998.
- 493 Humbert, G., Jaffrezic, A., Fovet, O., Gruau, G., and Durand, P.: Dry-season length and runoff control annual variability in stream  
494 DOC dynamics in a small, shallow groundwater-dominated agricultural watershed, *Water Resources Research*, 51, 7860-  
495 7877, <https://doi.org/10.1002/2015WR017336>, 2015.
- 496 Inamdar, S. P., O'Leary, N., Mitchell, M. J., and Riley, J. T.: The impact of storm events on solute exports from a glaciated forested  
497 watershed in western New York, USA, *Hydrological Processes*, 20, 3423-3439, <https://doi.org/10.1002/hyp.6141>, 2006.
- 498 Josse, J.: Principal component methods - hierarchical clustering - partitional clustering: why would we need to choose for  
499 visualizing data?,  
500 Kelly, D. J., Clare, J. J., and Bothwell, M. L.: Attenuation of solar ultraviolet radiation by dissolved organic matter alters benthic  
501 colonization patterns in streams, *Journal of the North American Benthological Society*, 20, 96-108, 10.2307/1468191, 2001.
- 502 Knorr, K. H.: DOC-dynamics in a small headwater catchment as driven by redox fluctuations and hydrological flow paths – are  
503 DOC exports mediated by iron reduction/oxidation cycles?, *Biogeosciences*, 10, 891-904, 10.5194/bg-10-891-2013, 2013.
- 504 Kothawala, D. N., Ji, X., Laudon, H., Ågren, A. M., Futter, M. N., Köhler, S. J., and Tranvik, L. J.: The relative influence of land  
505 cover, hydrology, and in-stream processing on the composition of dissolved organic matter in boreal streams, *Journal of  
506 Geophysical Research: Biogeosciences*, 120, 1491-1505, <https://doi.org/10.1002/2015.JG002946>, 2015.
- 507 Lambert, T., Perolo, P., Escoffier, N., and Perga, M. E.: Enhanced bioavailability of dissolved organic matter (DOM) in human-  
508 disturbed streams in Alpine fluvial networks, *Biogeosciences*, 19, 187-200, 10.5194/bg-19-187-2022, 2022.
- 509 Lambert, T., Pierson-Wickmann, A.-C., Gruau, G., Thibault, J.-N., and Jaffrezic, A.: Carbon isotopes as tracers of dissolved  
510 organic carbon sources and water pathways in headwater catchments, *Journal of Hydrology*, 402, 228-238,  
511 <https://doi.org/10.1016/j.jhydrol.2011.03.014>, 2011.
- 512 Lambert, T., Bouillon, S., Darchambeau, F., Morana, C., Roland, F. A. E., Descy, J.-P., and Borges, A. V.: Effects of human land  
513 use on the terrestrial and aquatic sources of fluvial organic matter in a temperate river basin (The Meuse River, Belgium),  
514 *Biogeochemistry*, 136, 191-211, 10.1007/s10533-017-0387-9, 2017.
- 515 Lambert, T., Pierson-Wickmann, A.-C., Gruau, G., Jaffrezic, A., Petitjean, P., Thibault, J.-N., and Jeanneau, L.: Hydrologically  
516 driven seasonal changes in the sources and production mechanisms of dissolved organic carbon in a small lowland  
517 catchment, *Water Resources Research*, 49, 5792-5803, <https://doi.org/10.1002/wrcr.20466>, 2013.
- 518 Lambert, T., Pierson-Wickmann, A. C., Gruau, G., Jaffrezic, A., Petitjean, P., Thibault, J. N., and Jeanneau, L.: DOC sources and  
519 DOC transport pathways in a small headwater catchment as revealed by carbon isotope fluctuation during storm events,  
520 *Biogeosciences*, 11, 3043-3056, 10.5194/bg-11-3043-2014, 2014.
- 521 Lê, S., Josse, J., and Husson, F.: FactoMineR: An R Package for Multivariate Analysis, *Journal of Statistical Software*, 25, 1 - 18,  
522 10.18637/jss.v025.i01, 2008.
- 523 Logozzo, L. A., Hosen, J. D., McArthur, J., and Raymond, P. A.: Distinct drivers of two size fractions of operationally dissolved  
524 iron in a temperate river, *Limnology and Oceanography*, 68, 1185-1200, <https://doi.org/10.1002/lno.12338>, 2023.
- 525 Logozzo, L. A., Martin, J. W., McArthur, J., and Raymond, P. A.: Contributions of Fe(III) to UV-Vis absorbance in river water: a  
526 case study on the Connecticut River and argument for the systematic tandem measurement of Fe(III) and CDOM,  
527 *Biogeochemistry*, 160, 17-33, 10.1007/s10533-022-00937-5, 2022.
- 528 Lotfi-Kalahroodi, E., Pierson-Wickmann, A.-C., Rouxel, O., Marsac, R., Bounnik-Le Coz, M., Hanna, K., and Davranche, M.: More  
529 than redox, biological organic ligands control iron isotope fractionation in the riparian wetland, *Scientific Reports*, 11, 1933,  
530 10.1038/s41598-021-81494-z, 2021.
- 531 Lucassen, E. C. H. E. T., Smolders, A. J. P., van der Salm, A. L., and Roelofs, J. G. M.: High groundwater nitrate concentrations  
532 inhibit eutrophication of sulphate-rich freshwater wetlands, *Biogeochemistry*, 67, 249-267,  
533 10.1023/B:BIOG.0000015342.40992.cb, 2004.
- 534 McMahon, P. B. and Chapelle, F. H.: Redox Processes and Water Quality of Selected Principal Aquifer Systems, *Groundwater*,  
535 46, 259-271, <https://doi.org/10.1111/j.1745-6584.2007.00385.x>, 2008.



- 536 Mehring, A. S., Lowrance, R. R., Helton, A. M., Pringle, C. M., Thompson, A., Bosch, D. D., and Vellidis, G.: Interannual drought  
537 length governs dissolved organic carbon dynamics in blackwater rivers of the western upper Suwannee River basin, *Journal*  
538 *of Geophysical Research: Biogeosciences*, 118, 1636-1645, <https://doi.org/10.1002/2013JG002415>, 2013.
- 539 Molenat, J., Gascuel-Oudou, C., Ruiz, L., and Gruau, G.: Role of water table dynamics on stream nitrate export and concentration  
540 in agricultural headwater catchment (France), *Journal of Hydrology*, 348, 363-378,  
541 <https://doi.org/10.1016/j.jhydrol.2007.10.005>, 2008.
- 542 Monteith, D. T., Stoddard, J. L., Evans, C. D., de Wit, H. A., Forsius, M., Högåsen, T., Wilander, A., Skjelkvåle, B. L., Jeffries, D.  
543 S., Vuorenmaa, J., Keller, B., Kopáček, J., and Vesely, J.: Dissolved organic carbon trends resulting from changes in  
544 atmospheric deposition chemistry, *Nature*, 450, 537-540, 10.1038/nature06316, 2007.
- 545 Murphy, K. R., Stedmon, C. A., Graeber, D., and Bro, R.: Fluorescence spectroscopy and multi-way techniques. PARAFAC,  
546 *Analytical Methods*, 5, 6557-6566, 10.1039/C3AY41160E, 2013.
- 547 Murphy, K. R., Stedmon, C. A., Wenig, P., and Bro, R.: OpenFluor— an online spectral library of auto-fluorescence by organic  
548 compounds in the environment, *Analytical Methods*, 6, 658-661, 10.1039/C3AY41935E, 2014.
- 549 Musolf, A., Selle, B., Büttner, O., Opitz, M., and Tittel, J.: Unexpected release of phosphate and organic carbon to streams linked  
550 to declining nitrogen depositions, *Global Change Biology*, 23, 1891-1901, <https://doi.org/10.1111/gcb.13498>, 2017.
- 551 Ohno, T.: Fluorescence Inner-Filtering Correction for Determining the Humification Index of Dissolved Organic Matter,  
552 *Environmental Science & Technology*, 36, 742-746, 10.1021/es0155276, 2002.
- 553 Pacific, V. J., Jencso, K. G., and McGlynn, B. L.: Variable flushing mechanisms and landscape structure control stream DOC  
554 export during snowmelt in a set of nested catchments, *Biogeochemistry*, 99, 193-211, 10.1007/s10533-009-9401-1, 2010.
- 555 Poulin, B. A., Ryan, J. N., and Aiken, G. R.: Effects of Iron on Optical Properties of Dissolved Organic Matter, *Environmental*  
556 *Science & Technology*, 48, 10098-10106, 10.1021/es502670r, 2014.
- 557 Raymond, P. A. and Saiers, J. E.: Event controlled DOC export from forested watersheds, *Biogeochemistry*, 100, 197-209,  
558 10.1007/s10533-010-9416-7, 2010.
- 559 Ruckhaus, M., Seybold, E. C., Underwood, K. L., Stewart, B., Kincaid, D. W., Shanley, J. B., Li, L., and Perdrial, J. N.:  
560 Disentangling the responses of dissolved organic carbon and nitrogen concentrations to overlapping drivers in a northeastern  
561 United States forested watershed, *Frontiers in Water*, 5, 10.3389/frwa.2023.1065300, 2023.
- 562 Sanderman, J., Lohse, K. A., Baldock, J. A., and Amundson, R.: Linking soils and streams: Sources and chemistry of dissolved  
563 organic matter in a small coastal watershed, *Water Resources Research*, 45, <https://doi.org/10.1029/2008WR006977>, 2009.
- 564 Selle, B., Knorr, K.-H., and Lischeid, G.: Mobilisation and transport of dissolved organic carbon and iron in peat catchments—  
565 Insights from the Lehstenbach stream in Germany using generalised additive models, *Hydrological Processes*, 33, 3213-  
566 3225, <https://doi.org/10.1002/hyp.13552>, 2019.
- 567 Škerlep, M., Nehzati, S., Sponseller, R. A., Persson, P., Laudon, H., and Kritzbeg, E. S.: Differential Trends in Iron Concentrations  
568 of Boreal Streams Linked to Catchment Characteristics, *Global Biogeochemical Cycles*, 37, e2022GB007484,  
569 <https://doi.org/10.1029/2022GB007484>, 2023.
- 570 Smith, G. J., McDowell, R. W., Condon, L. M., Daly, K., Ó hUallacháin, D., and Fenton, O.: Reductive dissolution of phosphorus  
571 associated with iron-oxides during saturation in agricultural soil profiles, *Journal of Environmental Quality*, 50, 1207-1219,  
572 <https://doi.org/10.1002/eq2.20256>, 2021.
- 573 Smolders, E., Baetens, E., Verbeeck, M., Nawara, S., Diels, J., Verdriev, M., Peeters, B., De Cooman, W., and Baken, S.: Internal  
574 Loading and Redox Cycling of Sediment Iron Explain Reactive Phosphorus Concentrations in Lowland Rivers, *Environmental*  
575 *Science & Technology*, 51, 2584-2592, 10.1021/acs.est.6b04337, 2017.
- 576 Stedmon, C. A. and Markager, S.: Resolving the variability in dissolved organic matter fluorescence in a temperate estuary and  
577 its catchment using PARAFAC analysis, *Limnology and Oceanography*, 50, 686-697,  
578 <https://doi.org/10.4319/lo.2005.50.2.0686>, 2005.
- 579 Strohmenger, L., Fovet, O., Akkal-Corfini, N., Dupas, R., Durand, P., Faucheux, M., Gruau, G., Hamon, Y., Jaffrezic, A., Minaudo,  
580 C., Petitjean, P., and Gascuel-Oudou, C.: Multitemporal Relationships Between the Hydroclimate and Exports of Carbon,  
581 Nitrogen, and Phosphorus in a Small Agricultural Watershed, *Water Resources Research*, 56, e2019WR026323,  
582 <https://doi.org/10.1029/2019WR026323>, 2020.
- 583 Tiwari, T., Sponseller, R. A., and Laudon, H.: The emerging role of drought as a regulator of dissolved organic carbon in boreal  
584 landscapes, *Nature Communications*, 13, 5125, 10.1038/s41467-022-32839-3, 2022.
- 585 Turgeon, J. M. L. and Courchesne, F.: Hydrochemical behaviour of dissolved nitrogen and carbon in a headwater stream of the  
586 Canadian Shield: relevance of antecedent soil moisture conditions, *Hydrological Processes*, 22, 327-339,  
587 <https://doi.org/10.1002/hyp.6613>, 2008.
- 588 Vázquez, E., Romani, A. M., Sabater, F., and Butturini, A.: Effects of the Dry–Wet Hydrological Shift on Dissolved Organic Carbon  
589 Dynamics and Fate Across Stream–Riparian Interface in a Mediterranean Catchment, *Ecosystems*, 10, 239-251,  
590 10.1007/s10021-007-9016-0, 2007.
- 591 Wen, H., Perdrial, J., Abbott, B. W., Bernal, S., Dupas, R., Godsey, S. E., Harpold, A., Rizzo, D., Underwood, K., Adler, T., Sterle,  
592 G., and Li, L.: Temperature controls production but hydrology regulates export of dissolved organic carbon at the catchment  
593 scale, *Hydrol. Earth Syst. Sci.*, 24, 945-966, 10.5194/hess-24-945-2020, 2020.
- 594 Werner, B. J., Musolf, A., Lechtenfeld, O. J., de Rooij, G. H., Oosterwoud, M. R., and Fleckenstein, J. H.: High-frequency  
595 measurements explain quantity and quality of dissolved organic carbon mobilization in a headwater catchment,  
596 *Biogeosciences*, 16, 4497-4516, 10.5194/bg-16-4497-2019, 2019.
- 597 Wetzel, R. G.: Gradient-dominated ecosystems: sources and regulatory functions of dissolved organic matter in freshwater  
598 ecosystems, *Hydrobiologia*, 229, 181-198, 10.1007/BF00007000, 1992.
- 599 Williams, C. J., Yamashita, Y., Wilson, H. F., Jaffé, R., and Xenopoulos, M. A.: Unraveling the role of land use and microbial  
600 activity in shaping dissolved organic matter characteristics in stream ecosystems, *Limnology and Oceanography*, 55, 1159-  
601 1171, <https://doi.org/10.4319/lo.2010.55.3.1159>, 2010.
- 602 Xu, N. and Saiers, J. E.: Temperature and Hydrologic Controls on Dissolved Organic Matter Mobilization and Transport within a  
603 Forest Topsoil, *Environmental Science & Technology*, 44, 5423-5429, 10.1021/es1002296, 2010.
- 604 Yamashita, Y., Scinto, L. J., Maie, N., and Jaffé, R.: Dissolved Organic Matter Characteristics Across a Subtropical Wetland's  
605 Landscape: Application of Optical Properties in the Assessment of Environmental Dynamics, *Ecosystems*, 13, 1006-1019,  
606 10.1007/s10021-010-9370-1, 2010.
- 607 Zarnetske, J. P., Bouda, M., Abbott, B. W., Saiers, J., and Raymond, P. A.: Generality of Hydrologic Transport Limitation of  
608 Watershed Organic Carbon Flux Across Ecoregions of the United States, *Geophysical Research Letters*, 45, 11,702-711,711,  
609 <https://doi.org/10.1029/2018GL080005>, 2018.



610

611 **Figure Caption**

612 **Figure 1** – Location map of the Kervidy-Naizin experimental catchment. Grey areas located  
613 along the stream channel network indicate the extent of hydromorphic soils commonly  
614 waterlogged during the winter period. Soil waters were located downslope the piezometer PK1.

615 **Figure 2** – A) Record of hourly discharge and daily rainfall, B) record of hourly piezometric  
616 levels in wetland (PK1) and upland (PK3) domains, and C) record of daily air temperature.  
617 Black triangles in panel A indicate fieldwork for manual sampling of soil and stream waters.

618 **Figure 3** – Evolution of (A) temperature, (B) pH, (C) DOC, (D) nitrates, (E) iron, and (F) SRP  
619 in soil waters during the study period.

620 **Figure 4** – Relationships between (A) DOC and iron, (B) iron and nitrates, ad (C) SRP and  
621 iron in soil waters during the study period.

622 **Figure 5** – PCA biplot, including loadings plot for the input variables and scores plot for  
623 lysimeters. One point represents one lysimeters, PCA being based on average values  
624 calculated over the study period. Markers are coloured according to the cluster identified by  
625 the Hierarchical Clustering on Principal Components (see material and methods).

626 **Figure 6** – Evolution of (A) DOC, (B) iron, (C) nitrates, and (D) SRP in soil waters. Lysimeters  
627 are grouped according the Hierarchical Clustering on Principal Components (Fig. 5).

628 **Figure 7** – Evolution of stream DOC measured at the outlet of the catchment. Variations in soil  
629 DOC concentrations grouped by cluster are also plotted for comparison.

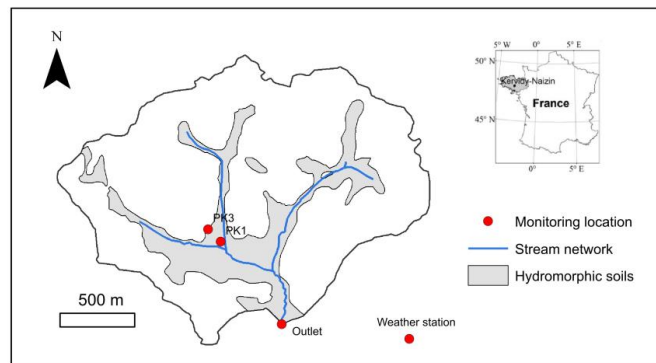
630

631





632 **Figure 1**

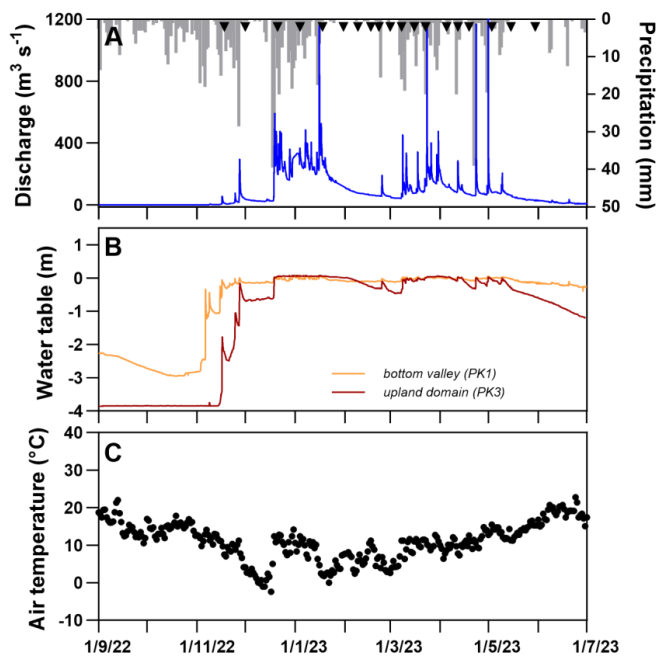


633

634



635 **Figure 2**

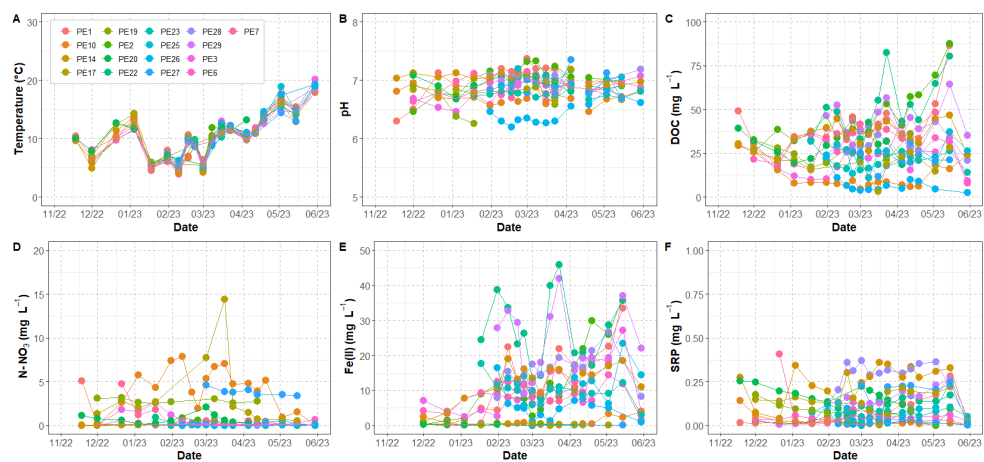


636

637



638 **Figure 3**

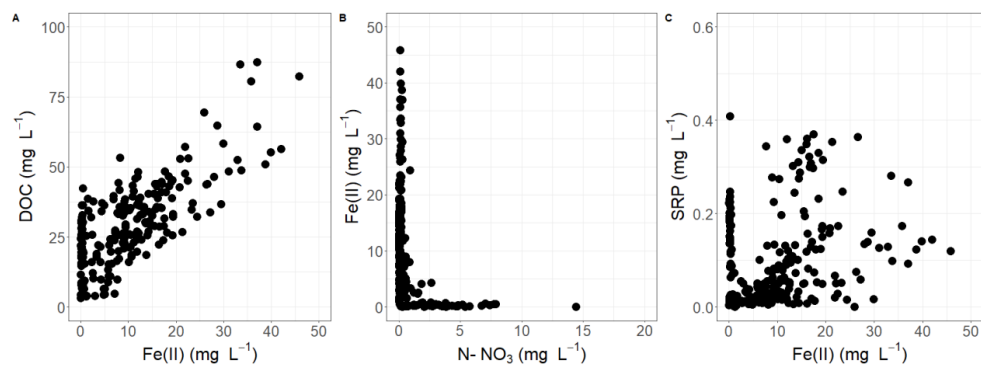


639

640



641 **Figure 4**

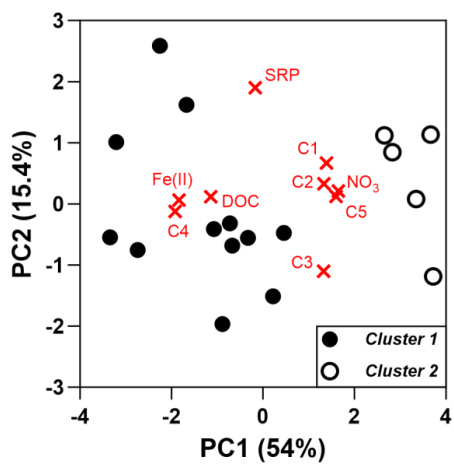


642

643



644 **Figure 5**

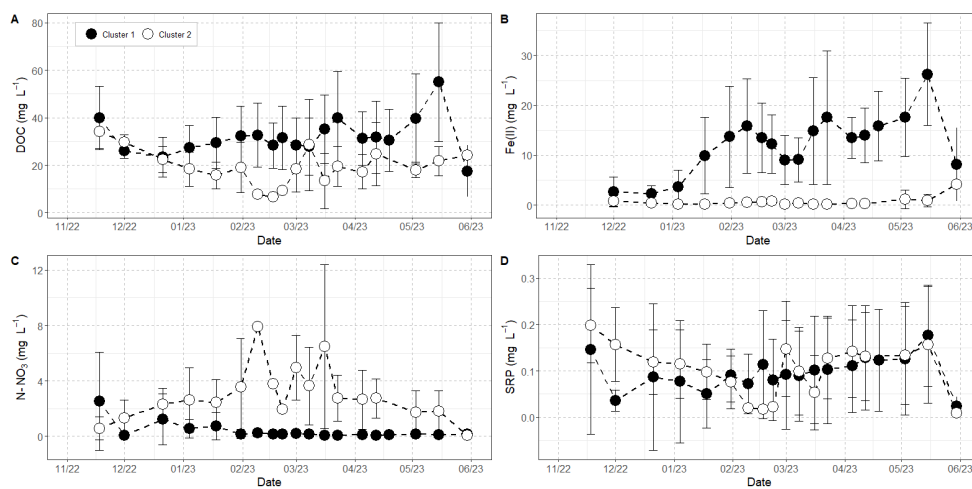


645

646



647 **Figure 6**

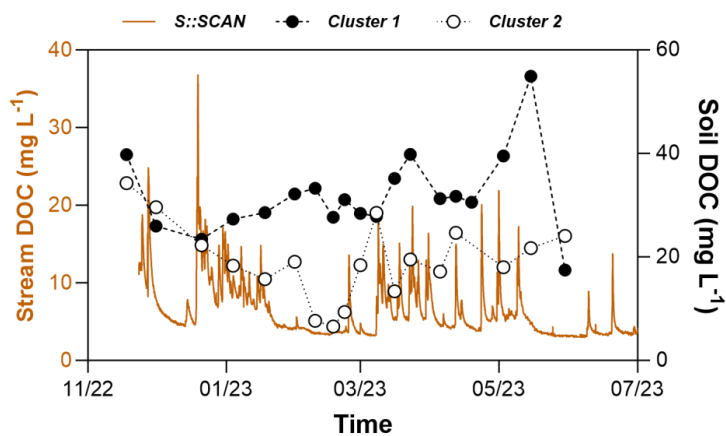


648

649



650 **Figure 7**



651